Effect of Geogrid Reinforcement on Railroad Ballast Performance Evaluated through Triaxial Testing and Discrete Element Modeling

Yu Qian[1], Erol Tutumluer[2], M. ASCE, Debakanta Mishra[3] and Hasan Kazmee[4]

[1]Graduate Research Assistant, Department of Civil and Environmental Engineering, University of Illinois at Urbana-Champaign, Urbana, IL, 61801, yuqian1@illinois.edu
[2]Professor and Corresponding Author, Department of Civil and Environmental Engineering, University of Illinois at Urbana-Champaign, Urbana, IL, 61801, 217-333-8637, tutumlue@illinois.edu
[3]Post-Doctoral Research Associate, Department of Civil and Environmental Engineering, University of Illinois at Urbana-Champaign, Urbana, IL, 61801, dmishra2@illinois.edu
[4]Graduate Research Assistant, Department of Civil and Environmental Engineering, University of Illinois at Urbana-Champaign, Urbana, IL, 61801, kazmee2@illinois.edu

ABSTRACT: Geogrids have been found to effectively improve the performance of unbound aggregate layers in transportation applications by providing confinement and arresting movement through interlock between individual aggregate particles and their apertures. Geogrid reinforcement offers an effective remedial measure when railroad track structures are susceptible to track geometry defects resulting from excessive movement and particle reorientation within the ballast layer. This paper presents an ongoing research study at the University of Illinois aimed at quantifying the effects of geogrid reinforcement on the shear strength and permanent deformation behavior of railroad ballast. Geogrids with triangular, rectangular, and square apertures were tested in the laboratory experiments. Cylindrical ballast specimens were prepared and tested with geogrids placed at different heights within the specimen using a large-scale triaxial apparatus. An imaging based Discrete Element Method (DEM) modeling approach was developed to model triaxial test results and investigate geogrid reinforcement mechanisms. With the capability to create actual ballast aggregate particles as three-dimensional polyhedron elements having the same particle size distributions and imaging quantified average shapes and angularities, the DEM simulations were able to capture the ballast behavior with and without geogrid reinforcement reasonably accurately.

INTRODUCTION

Geogrids are commonly used in railway track construction for ballast and sub-ballast stabilization purposes. Due to the particulate nature of ballast particles, geogrids can be placed within the ballast layer to improve strength and modulus properties of ballast layer, limit lateral movement of ballast particles, and reduce vertical settlement through effective geogrid-aggregate interlocking. What dictates the geogrid location within a ballast/subballast layer in the field is often the depth below which tamping arms or tines of ballast tamping equipment cannot reach during routine railroad maintenance activities. However, the optimal location to install geogrids in ballast layer has not been thoroughly studied.

Previous studies have already concluded biaxial geogrids, often with rectangular or square apertures, to be quite effective for improving bearing capacity of the track

substructure through laboratory tests or numerical simulations (Bathurst and Raymond 1987, Shin et al. 2002, Raymond and Ismail 2003, Indraratna et al. 2006, Brown et al. 2007, Kwon and Penman 2009, Qian et al. 2011a). However, biaxial geogrids only have high tensile strength properties mainly in two directions, machine direction and cross-machine direction, which limits the benefit of reinforcement. More recently, geogrids with triangular shaped apertures have also been developed with the claims to provide more uniform reinforcement in all directions. An early work on comparative modeling evaluation of the reinforcement benefits of geogrids with rectangular and triangular geogrids was offered by Tutumluer et al. (2009a) through discrete element modeling simulations of direct shear tests. Recent research efforts have also focused on evaluating performance improvements of triangular geogrid reinforced transportation systems (Qian et al. 2011b, Qian et al. 2013,).

This paper describes preliminary findings from an ongoing research study at the University of Illinois focusing on triaxial testing of geogrid-reinforced ballast specimens using a large scale triaxial test device and modeling the micromechanical interlock behavior of geogrid-aggregate systems with the Discrete Element Method (DEM). Ballast specimens reinforced with geogrids having triangular or square apertures were tested under three different configurations to evaluate the reinforcement benefits through improved stress-strain behavior and strength properties. Ballast specimens reinforced by a single layer of geogrid at middle of the specimen were tested to evaluate the reinforcement benefits through repeated loading and permanent deformation tests. Unreinforced ballast specimens were also tested as the control samples for the strength and permanent deformation evaluations. To simulate the triaxial tests and investigate geogrid reinforcement mechanisms, a numerical modeling approach based on the DEM was adopted with the capability to create actual ballast aggregate particles as three-dimensional polyhedron elements having the same particle size distributions and imaging quantified average shapes and angularities. Both the triaxial strength tests and the DEM simulation results are presented to evaluate the reinforcement benefits and mechanisms governing behavior of the ballast specimens reinforced with different aperture geogrids.

TRIAXIAL TESTS OF BALLAST SPECIMENS

A large scale triaxial test device (The University of Illinois Ballast Triaxial Tester or TX-24) was recently developed at the University of Illinois for testing specifically ballast size aggregate materials. The test specimen dimensions are 30.5 cm (12 in.) in diameter and 61.0 cm (24 in.) in height. An internal load cell (Honeywell Model 3174) with a capacity of 89 kN (20 kips) is placed on top of the specimen top platen. Three vertical LVDTs are placed around the cylindrical test specimen at 120-degree angles between each other to measure the vertical deformations of the specimen from three different side locations. Another LVDT is mounted on a circumferential chain wrapped around the specimen at the mid-height to measure the radial deformation of the test specimen. Fig. 1 shows a photo of the TX-24 setup having an instrumented ballast specimen ready for testing.

FIG. 1. The University of Illinois ballast triaxial tester (TX-24)

Considering realistically the influence of traffic induced rather high loading rates on the ballast material behavior, laboratory triaxial strength tests were conducted at a rapid shearing rate of 5% strain per second at an applied constant confining pressure of 138 kPa (20 psi). A similar approach was proposed by Garg and Thompson (1997) to evaluate strength properties of granular materials under vehicle loading. Considering the 61.0-cm (24-in.) high ballast specimens, these loading rates correspond to vertical ram movements of 30.5 mm (1.2 in.) per second. Due to the large movements of the loading ram causing instant bulging and shearing of ballast samples, the LVDTs were not used during the ballast strength tests but only during permanent deformation tests. For the permanent deformation tests, a repeated type haversine pulse loading with a peak deviator stress of 165 kPa (24 psi) was applied at a constant confining pressure of 55 kPa (8 psi). Each loading pulse lasted 0.4 seconds and there was a 0.6-second rest period applied between the two pulse loadings.

The ballast material used in the triaxial strength tests was a clean limestone having 100% crushed aggregates. Fig. 2 shows the size distribution of the ballast material which adequately met the US AREMA No. 24 gradation requirements. Besides the grain size distribution, aggregate shape properties, especially the flat and elongated (F&E) ratio, the angularity index (AI), and the surface texture (ST) index, are key indices quantified by the University of Illinois Aggregate Image Analyzer (UIAIA) (Rao et al. 2002). One full bucket of the ballast material was scanned and analyzed using the recently enhanced E-UIAIA to determine the values of the F&E ratio, AI, and ST index, which were then used as the essential morphological data to generate ballast aggregate particle shapes as three-dimensional (3D) polyhedrons, i.e., individual discrete elements utilized in the ballast DEM model (see Fig. 3).

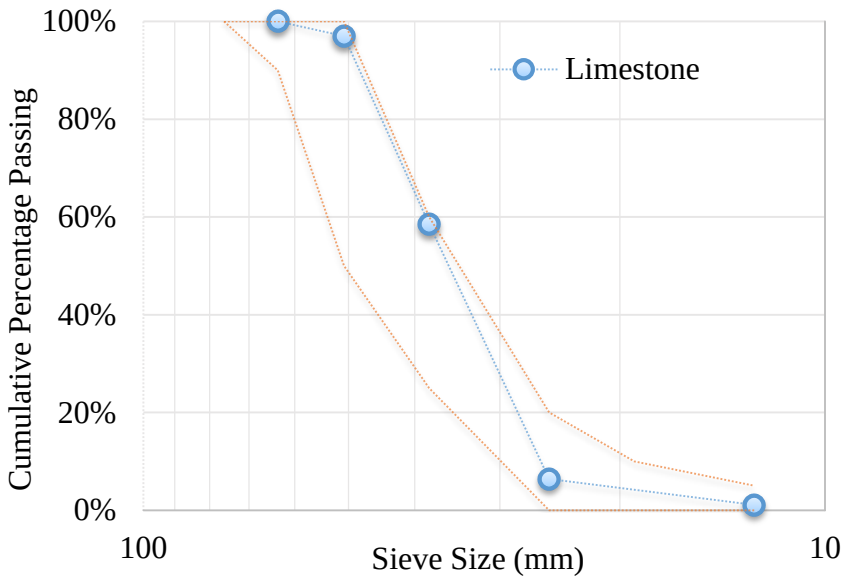

FIG. 2. Particle size distribution of limestone ballast aggregate compared to U.S. AREMA No. 24 specifications

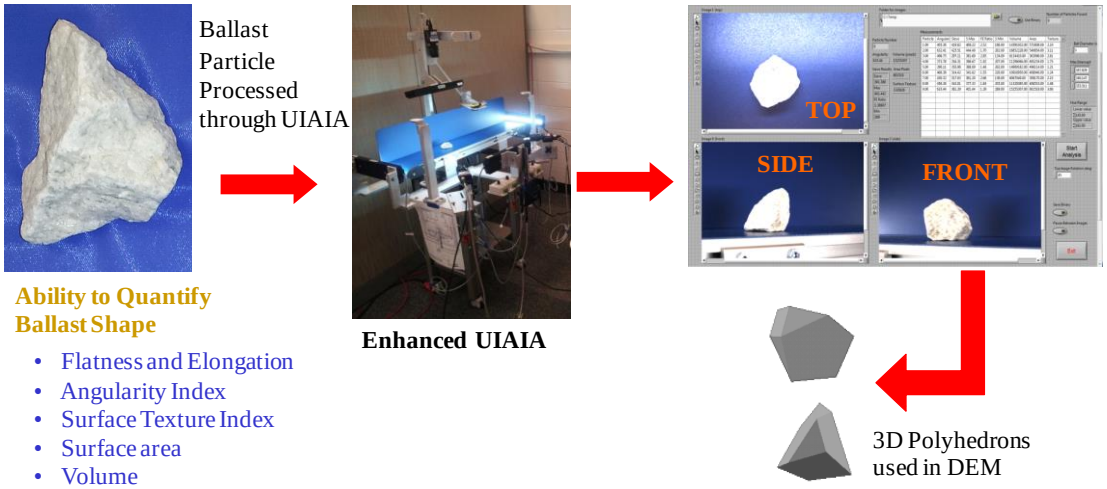

FIG. 3. Conceptual approach for aggregate imaging based railroad ballast particle generation for discrete element method (DEM) simulations

Approximately 68 to 73 kg (150 to 160 lbs) of ballast material was poured into an aluminum split mold in several lifts, and compacted using a 27.2-kg (60-lb.) electric jack hammer for approximately 16 seconds. The thickness of each lift and corresponding compaction time were calculated to ensure uniform and even compaction based on where geogrid was placed. After compaction of specimen to desired depth, geogrid was placed into the test specimen. Fig. 4 shows the aluminum split mold, geogrids used in this study with their locations marked in a prepared

specimen ready for test, and geogrids placed in the specimen. During the permanent deformation test, only a single layer of geogrid was placed at the middle of the specimen, which is also referred to as configuration (a). At the end of placing all lifts and geogrid(s), each test specimen was checked for the total height and leveling of the top plate. The void ratios (e) computed were consistently around 0.68. Although placing two layers of geogrid within the ballast layer is not often practical and may not be cost effective in the field, the two layers of geogrids installed in the test specimens were intended to investigate in the laboratory the aggregate-geogrid interlock mechanism and sample bulging behavior through DEM modeling. The detailed properties of the geogrids used, ballast gradation and the average values of the limestone ballast UIAIA shape indices are given in Table 1.

TABLE 1. Properties of Ballast Aggregate and Geogrids Used

Ballast Material (Limestone) Properties					
Angularity Index (AI) in degrees	Flat & Elongation (F&E) Ratio	Surface Texture (ST) Index		Cu	Cc
440	2.3	2		1.46	0.97
Geogrid Properties					
	Square Aperture	Rectangular Aperture		Triangular Aperture	
	Side	Machine Direction	X-Machine Direction	Longitudinal	Diagonal
Aperture Dimensions (mm)	65	46	64	60	60
Ultimate QC Strength (kN/m)	30				
Junction Efficiency (percentage)		93		93	
Aperture Stability Modulus(m-N/deg)		0.58			
Radial stiffness (kN/m@0.5% strain)				350	

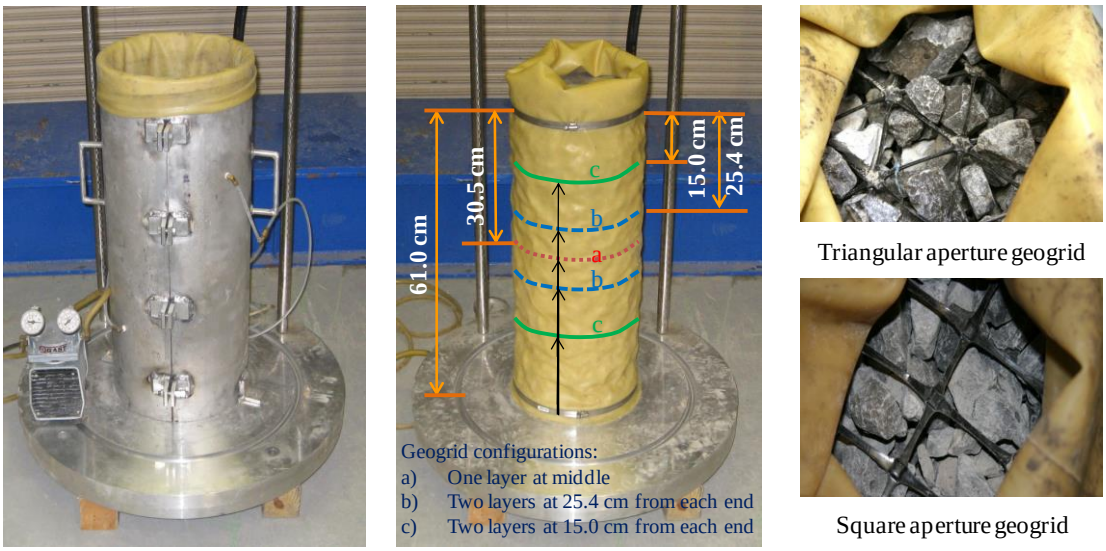

FIG. 4. Aluminum split mold, test specimen, and geogrids used in this study

DEM SIMULATIONS OF THE TRIAXIAL TESTS

DEM model preparation

Discrete Element Method (DEM) is one of the most suitable numerical simulation approach to simulate a granular system that consisting of discrete particle. The DEM has already been successfully applied to simulate ballast behavior by using spherical elements or element clusters to represent ballast particles (Indraratna et al. 2010, Lu and McDowell 2010). The DEM simulation approach developed at the University of Illinois adopts real polyhedral particles and has the capability to create actual ballast aggregate particles as 3D polyhedron elements having the same particle size distributions and imaging quantified average shapes and angularities. This DEM approach was calibrated by the laboratory large scale direct shear test results for ballast size aggregate application (Tutumluer et al. 2006), and has been successfully utilized to simulate complex ballast behavior, such as: effects of multi-scale aggregate morphological properties, gradation, and fouling. (Tutumluer et al. 2006, 2007, 2008, 2009b). A successful field validation study was also completed to conclude that the DEM approach was quite adequate and reasonably accurate for predicting actual ballast layer deformation behavior (Tutumluer et al. 2013).

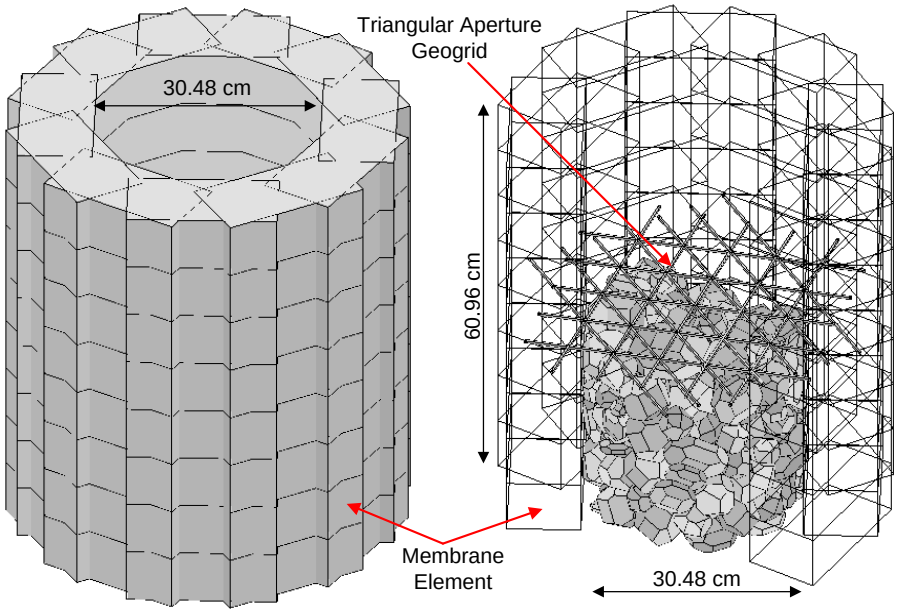

FIG. 5. Flexible membrane shown on left to model one layer geogrid reinforced triaxial ballast specimen established as a DEM simulation

Lee et al. (2012) recently used rigid rectangular cuboid discrete elements positioned in a cylindrical arrangement to simulate a flexible membrane with BLOKS3D DEM program. A similar approach was used in this study. A total of 96 rectangular cuboid discrete elements (in eight-layers) were used to form a cylindrical chamber to confine the ballast specimen as shown in Fig. 5. Each layer had 12 equal

sized elements and the dimension of each single element was 20.3 cm (8 in.) long, 10.2 cm (4 in.) wide, and 7.6 cm (3 in.) high. These membrane elements were only allowed translational movement in radial direction. Rotation and translation movement in other directions were restricted to replicate the deformation of the specimen membrane. In order to simulate the membrane behavior without applying extra confinement, the contact between membrane elements and the friction between the membrane elements and the ballast particles in contact were both ignored. The DEM simulations followed the same specimen preparation and loading steps of the laboratory tests. Due to brevity, only the triangular aperture-geogrid reinforced ballast tests simulated are presented in this paper.

LABORATORY TESTS AND DEM SIMULATION RESULTS

Fig. 6 presents the results of the large scale triaxial strength tests on the limestone ballast cylindrical specimens for up to 10% axial strain. All the test specimens showed similar stress-strain behavior at the initial small strain stage of the strength tests and this was primarily due to the fact that geogrids were not yet fully mobilized early on. When axial strain levels increased, the geogrid was mobilized and the interlock between geogrid and aggregate particles prevented lateral movement or specimen bulging. The zigzag shapes of the stress-strain curves at high axial strain levels indicate sudden strength drops. This can be explained by damaged geogrid due to observed broken ribs and/or particles reorienting themselves from the interlocked positions. Immediately afterwards, the geogrid-reinforced ballast was back to fully restrained condition again with new interlocks formed between aggregate particles and the geogrid and accordingly, the strength of the specimen was restored upon completion of the particle rearrangement. The DEM simulation results presented in Fig.6 (a) showed good agreement with the observed trends in the experiments.

It is very interesting to note that both the triangular and the square aperture geogrids present the same reinforcement configurations corresponding to the different configurations of geogrids placed in the specimens. Two geogrid layers placed at 25.4 cm from bottom and top of the specimen, respectively, presented the best performance from the experiments. However, no significant strength improvement was observed when two layers of geogrids were placed at 15.0 cm from bottom and top of the specimen, respectively. This confirmed that the reinforcement effect highly depends on the position where geogrid is placed in the specimen during the triaxial tests. Due to the interlock of the geogrid and aggregate particles, a local “stiffened or reinforced” zone can form in the location where the geogrid is placed (Qian et al 2011a). During triaxial shearing, the most severe bulging took place in the mid-specimen height for the unreinforced ballast sample. When the geogrid was placed in the mid-specimen height, the reinforcement effect was quite significant especially at large axial strain levels. However, if geogrid was placed too far away from the critical location, i.e., the mid-specimen, the specimen could not be effectively reinforced.

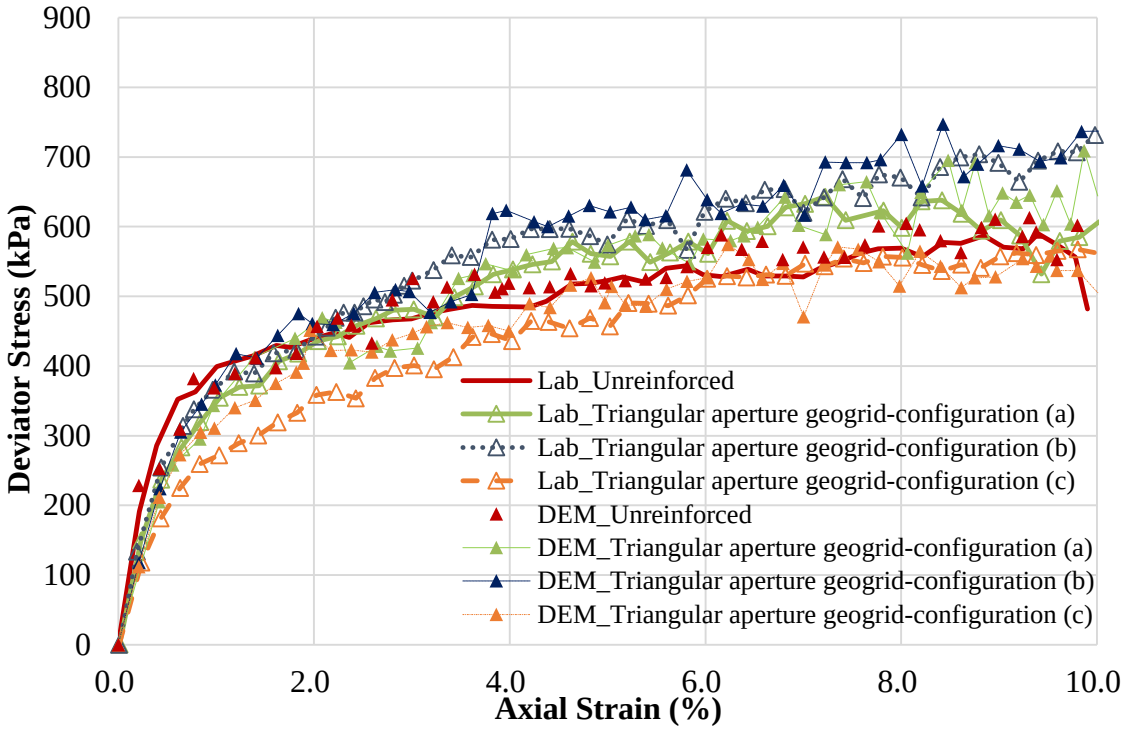

(a) Strength tests and DEM simulation results with triangular aperture geogrid

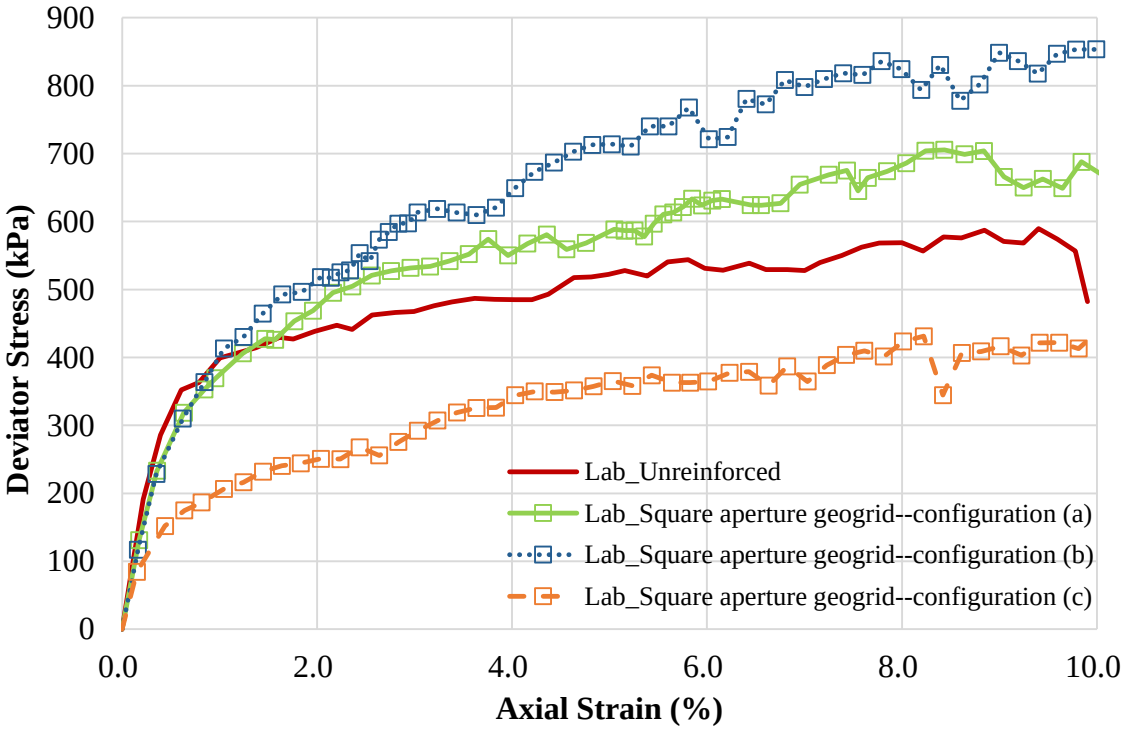

(b) Strength tests and DEM simulation results with square aperture geogrid

FIG. 6. Laboratory triaxial ballast strength tests and DEM simulation results

Fig. 7 presents the preliminary results of the ballast permanent deformation tests performed in the laboratory for up to 10,000 cycles. For the first several hundred loading cycles, the vertical and circumferential permanent deformations increased rapidly, which was primarily due to the initial rapid "shakedown" of the ballast material. After around 1,000 loading cycles, the permanent deformation accumulated much slower and became relatively stable, and so did the circumferential or radial/horizontal deformations. All the unreinforced and geogrid reinforced test specimens accumulated similar magnitudes of permanent deformation during the first one hundred load cycles and this was primarily due to the fact that geogrids were not yet fully mobilized at that time. With a single layer of geogrid placed in the middle of the test specimen, the geogrid reinforced test specimens accumulated less permanent deformation compared to the unreinforced case as the load cycles increased. When the reinforced test specimens accumulated a certain amount of deformation, the geogrid reinforcement effect was fully mobilized and the achieved interlock between geogrid and aggregate particles prevented specimen further bulging. This caused the specimen to stiffen and made it more resistant to deformation accumulation upon loading. Triangular aperture geogrid reinforced test specimen accumulated the smallest permanent deformation compared with the unreinforced as well as the specimen with rectangular aperture geogrid. This indicates that the triangular aperture geogrid better arrested aggregate movement with improved interlocking in all horizontal directions which can be confirmed from circumferential or radial/horizontal deformations, which happen to be of similar magnitude. Note that the triangular aperture geogrid also has thicker ribs and much higher radial stiffness when compared to the rectangular one.

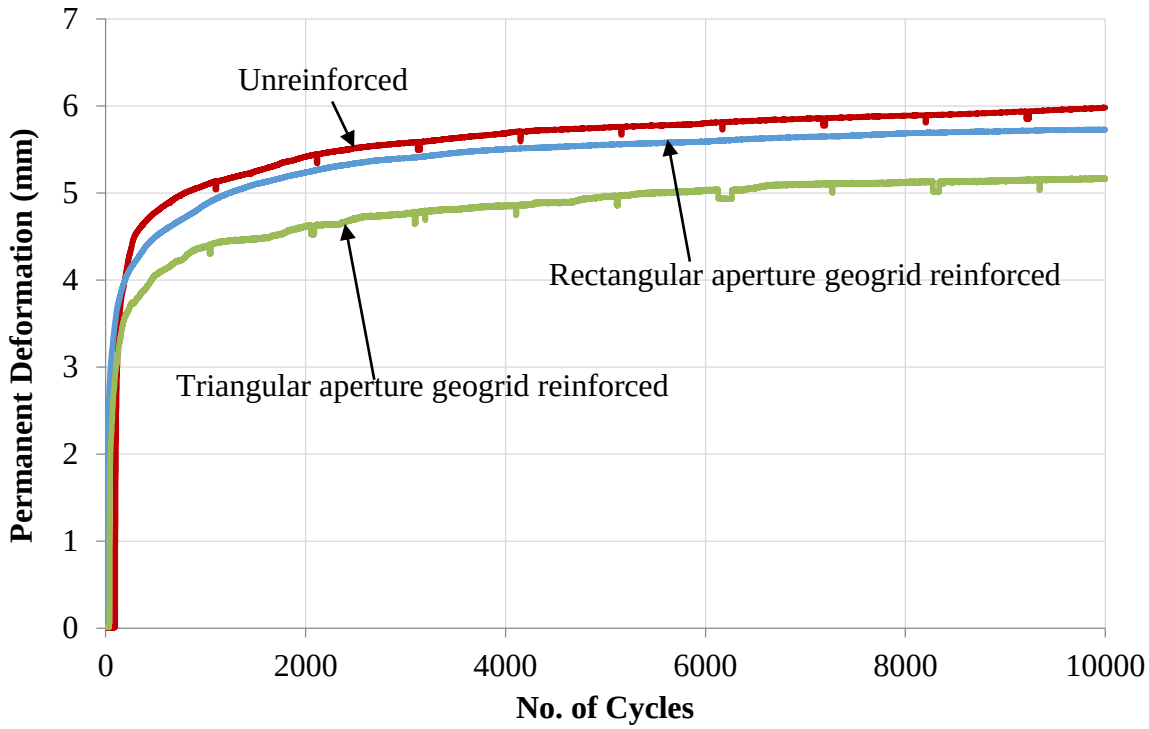

(a) Specimen permanent deformation in axial (vertical) direction

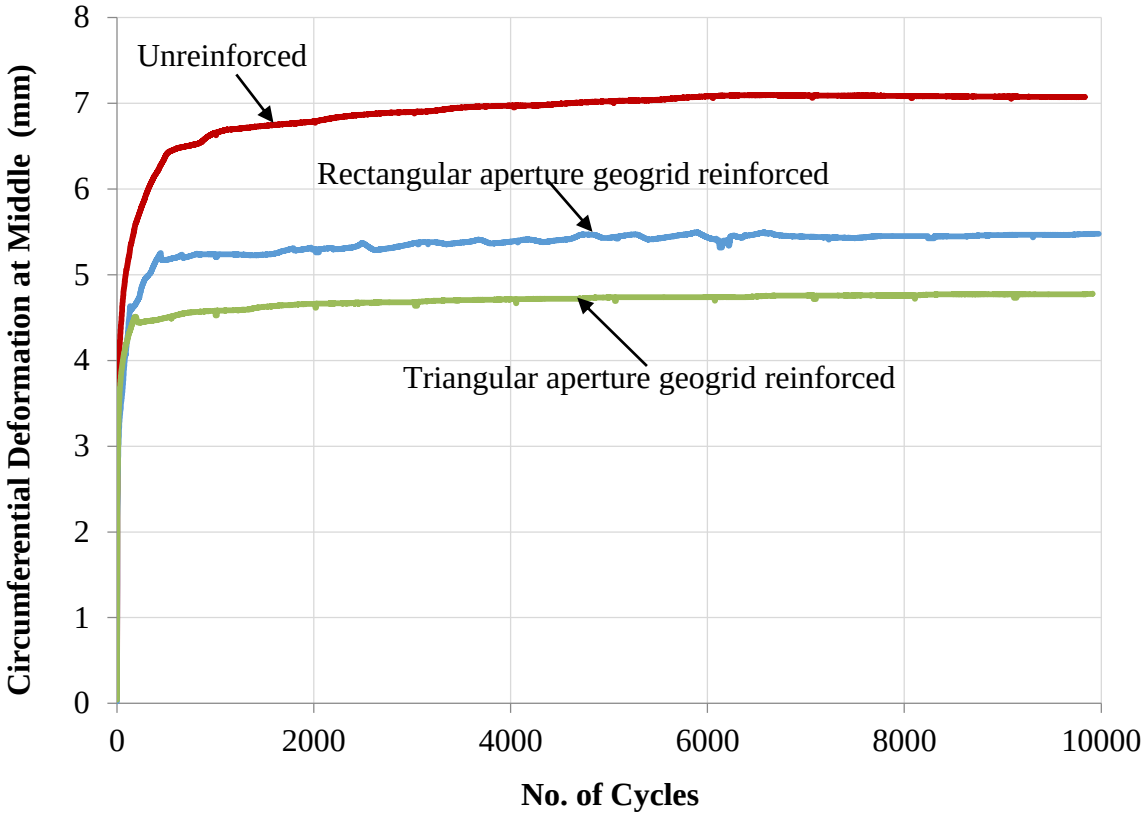

(b) Circumferential deformation at middle

FIG. 7. Ballast permanent deformations from repeated load triaxial tests

Fig. 8 presents permanent deformation predictions as computed by the DEM simulations for up to 100 load cycles. As the purpose of the DEM simulations was to qualitatively investigate the relative performance of geogrids with different aperture shapes, due to the long DEM run times associated with each loading case, the DEM simulations for the permanent deformation predictions here considered only up to 100 cycles of the load application. Although the permanent deformations for the first hundred load cycles were somewhat similar for the unreinforced and different geogrid reinforced specimens during the laboratory testing (see Fig. 7), with better control in compaction during specimen preparation in DEM simulations and the significantly high number of aggregate particle contact forces computed and checked for global granular assembly equilibrium at each iterative time step, a relatively low number of initial load cycles, such as 100 achieved here for three different simulation cases studied, was deemed to be sufficient for identifying the main reinforcement mechanisms and interlocking trends also identified in the experiments. Clearly, with DEM simulations of only up to 100 load cycles, the differences among the different ballast triaxial tests were apparent. The geogrid reinforced ballast specimens similarly yielded less permanent deformations compared to the unreinforced ballast specimen. The rectangular aperture geogrid did provide considerable reinforcement, but the triangular aperture geogrid with more uniform reinforcement in all horizontal

directions provided the most significant improvement as indicated in Fig. 8. These results from DEM simulations agree well with the trends observed in the laboratory experiments. It is interesting to note that the first five DEM simulation load cycles also yielded similar magnitude deformations for all the unreinforced and geogrid reinforced test specimens, which means the geogrids were not fully mobilized yet. However, as the load cycles increased, the triangular aperture geogrid started to show improvement at around the 8^{th} loading cycle during the simulation, while, the rectangular geogrid started to take effect at around the 16^{th} loading cycle (see Fig. 8). Again, the DEM simulations were intended to qualitatively compare the relative performances of geogrids with different aperture shapes using the minimum computational time. The intention has never been to match the predicted permanent deformation rates or the magnitudes at the different load cycles with the experimental results directly.

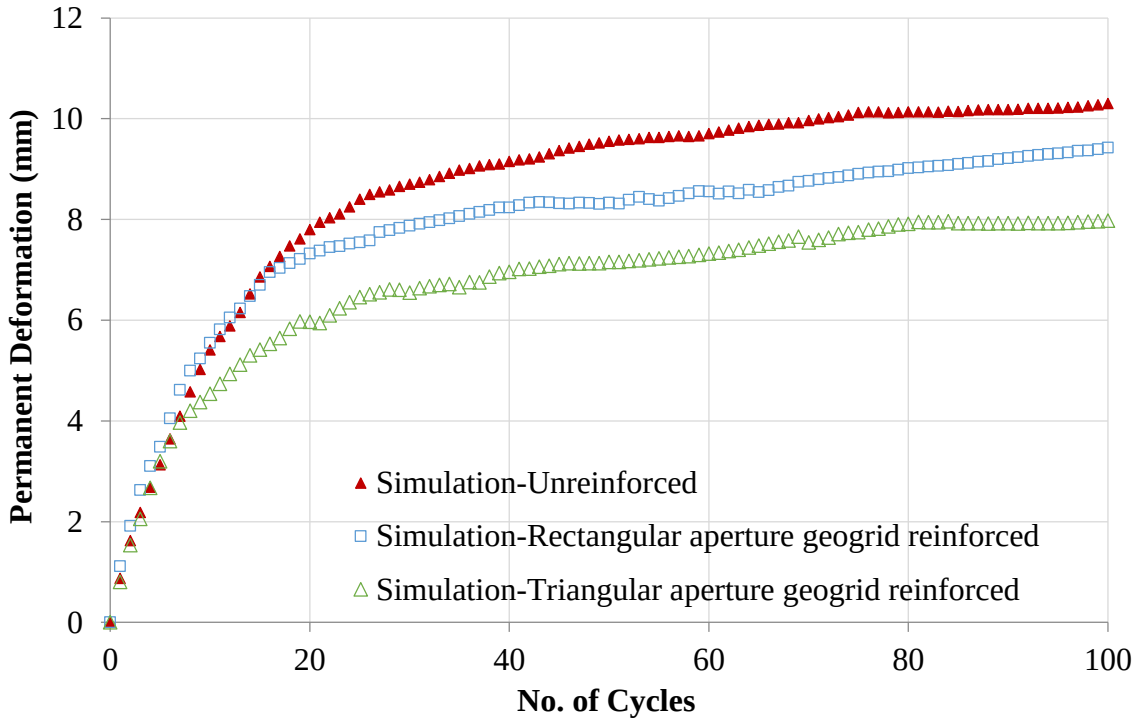

FIG. 8. DEM simulation results of permanent deformation tests

CONCLUSIONS

This paper focused on the shear strength and permanent deformation test results of geogrid reinforced ballast specimens as obtained from a large scale triaxial test device in the laboratory. Triangular, square, and rectangular aperture geogrids were used for ballast reinforcement. Numerical simulation was performed with an imaging based Discrete Element Method (DEM) modeling approach to demonstrate the capability of studying geogrid-aggregate interlock reinforcement mechanism and the

optimal reinforcement location of cylindrical test specimens in order to maximize strength properties. The following conclusions can be drawn from this study:

- The location of geogrid placement in a uniform sized aggregate assembly, such as railroad ballast, influences significantly the stress-strain behavior of cylindrical test specimen through creating different local "stiffened zones" and therefore reinforcement effects. Placing a single layer of geogrid at mid-specimen height, or two layers of geogrid close to the middle of the specimen where bulging takes place, provides better reinforcement benefits when compared to placing geogrid towards top and bottom, i.e., away from the middle of the test specimen, during triaxial strength testing. Both triangular aperture geogrid and square aperture geogrid presented the same reinforcement effect during monotonic strength test related to the different locations where geogrid was placed.
- Both rectangular and triangular aperture geogrids were found to effectively reduce the permanent deformation accumulations of ballast materials. Triangular aperture geogrid with uniform resistance in all horizontal directions yielded the lowest permanent deformation. More studies are needed to fully investigate aperture shape effects on the overall geogrid reinforcement mechanism.
- The aggregate imaging based DEM simulation platform developed at the University of Illinois could model the stress-strain behavior of ballast specimens under both monotonic and repeated load triaxial tests. The DEM simulation successfully captured the stress-strain behavior and deformation trends of the geogrid-reinforced ballast specimens by addressing adequately the initial condition of the laboratory tests. The DEM simulation platform currently being further developed has the potential for quantifying individual effects of various geogrid properties, such as aperture shape and size and rib dimensions, on the aggregate assembly.

REFERENCES

Bathurst, R. J. and Raymond, G. P., 1987. *Geogrid Reinforcement of Ballasted Track.* Transportation Research Record. No. 1153: 8-14.

Brown, S. F., Kwan, J. and Thom, N. H., 2007. *Identifying the Key Parameters that Influence Geogrid Reinforcement of Railway Ballast*. Geotextiles and Geomembranes, 25(6):326-335.

Garg, N. and Thompson, M.R., 1997. *Triaxial Characterization of Minnesota Road Research Project Granular Materials*. Journal of the Transportation Research Board. No.1577:27-36.

Indraratna, B., Khabbaz, H., Salim, W. and Christie, D., 2006. *Geotechnical Properties of Ballast and the Role of Geosynthetics in Rail Track Stabilisation.* Journal of Ground Improvement, 10(3): 91-102.

Indraratna, B., Thakur, P.K., and Vinod, J.S., 2010. *Experimental and Numerical Study of Railway Ballast Behavior under Cyclic Loading*. International Journal of Geomechanics, ASCE, 10(4):136-144.

Lee, S. J., Hashash, Y.M.A., and Nezami E.G., 2012. *Simulation of Triaxial Compression Test with Polyhedral Discrete Elements*. Computers and Geotechnics, in press.

Lu, M. and McDowell, G.R., 2010. *Discrete Element Modelling of Railway Ballast under Monotonic and Cyclic Triaxial Loading*. Geotechnique, 60(6):459-467.

Kwon, J. and Penman, J., 2009. *The Use of Biaxial Geogrids for Enhancing the Performance of Sub-Ballast and Ballast Layers—Previous Experience and Research*. 8th International Conference on Bearing Capacity of Roads, Railways and Airfields. June 29-July 2, Champaign, Illinois, USA.

Qian, Y., Tutumluer, E., and Huang, H., 2011a. *A Validated Discrete Element Modeling Approach for Studying Geogrid-Aggregate Reinforcement Mechanisms*. Geo-Frontiers 2011, ASCE Geo-Institute, March 13-16, Dallas, Texas.

Qian, Y., Han, J., and Pokharel, S.K., and Parsons, R.L., 2011b. *Stress Analysis on Triangular Aperture Geogrid-Reinforced Bases over Weak Subgrade under Cyclic Loading - An Experimental Study*. Journal of the Transportation Research Board, No. 2204, Low-Volume Roads, Vol. 2, Proceedings of the 10th International Conference on Low-Volume Roads, July 24–27, Lake Buena Vista, Florida, USA, 83-91.

Qian, Y., Han, J., and Pokharel, S.K., and Parsons, R.L., 2012. *Performance of Triangular Aperture Geogrid-Reinforced Base Courses over Weak Subgrade under Cyclic Loading*. Journal of Materials in Civil Engineering, in press.

Rao, C., Tutumluer, E. and Kim, I.T., 2002. *Quantification of Coarse Aggregate Angularity Based on Image Analysis*. Transportation Research Record. No. 1787, 193-201.

Raymond, G. and Ismail, I., 2003. *The Effect of Geogrid Reinforcement on Unbound Aggregates*. Geotextiles and Geomembranes, 21(6): pp.355-380.

Tutumluer, E., Huang, H., Hashash, Y.M.A., and Ghaboussi, J., 2006. *Aggregate Shape Effects on Ballast Tamping and Railroad Track Lateral Stability*. In Proceedings of the AREMA Annual Conference, Louisville, Kentucky, USA, September 17-20.

Tutumluer, E., Huang, H., Hashash, Y.M.A., and Ghaboussi, J., 2007. *Discrete Element Modeling of Railroad Ballast Settlement*. In Proceedings of the AREMA Annual Conference, Chicago, Illinois, September 9-12.

Tutumluer, E., Huang, H., Hashash, Y.M.A., and Ghaboussi, J., 2008. *Laboratory Characterization of Coal Dust Fouled Ballast Behavior*. In Proceedings of the AREMA Annual Conference, Salt Lake City, Utah, September 21-23.

Tutumluer, E, Huang, H., and Bian, X. 2009a. *Research on the Behavior of Geogrids in Stabilization Applications,* Proc., Jubilee Symposium on Polymer Geogrid Reinforcement, September 8, 2009, London, UK.

Tutumluer, E., Huang, H., Hashash, Y.M.A., and Ghaboussi, J., 2009b. *AREMA Gradations Affecting Ballast Performance Using Discrete Element Modeling (DEM) Approach*. In Proceedings of the AREMA Annual Conference, Chicago, Illinois, September 20-23.

Tutumluer, E., Qian, Y., Hashash, Y.M.A., Ghaboussi, J., and David, D.D., 2011. *Field Validated Discrete Element Model for Railroad Ballast*. In Proceedings of the AREMA Annual Conference, Minneapolis, Minnesota, September 18-21.